

引用格式: 刘军, 黄超, 周磊, 等, 2024. 基于阵列声波测井估算碳酸盐岩储层岩石力学和地应力参数: 以顺北 4 号带为例 [J]. 地质力学学报, 30 (3): 394-407. DOI: [10.12090/j.issn.1006-6616.2023110](https://doi.org/10.12090/j.issn.1006-6616.2023110)

Citation: LIU J, HUANG C, ZHOU L, et al., 2024. Estimation of the rock mechanics and in-situ stress parameters of carbonate reservoirs using array sonic logging: A case study of Shunbei No.4 block[J]. Journal of Geomechanics, 30 (3): 394-407. DOI: [10.12090/j.issn.1006-6616.2023110](https://doi.org/10.12090/j.issn.1006-6616.2023110)

基于阵列声波测井估算碳酸盐岩储层岩石力学和地应力参数 ——以顺北 4 号带为例

刘 军¹, 黄 超¹, 周 磊², 陈 群¹, 张生龙¹

LIU Jun¹, HUANG Chao¹, ZHOU Lei², CHEN Qun¹, ZHANG Shenglong¹

1. 中国石化西北油田分公司勘探开发研究院, 新疆 乌鲁木齐 830011;

2. 中国地质科学院地质力学研究所, 北京 100081

1. *Research Institute of Petroleum Exploration and Development, Northwest Oilfield Company, SINOPEC, Urumqi 830011, Xinjiang, China;*

2. *Institute of Geomechanics, Chinese Academy of Geological Sciences, Beijing 100081, China*

Estimation of the rock mechanics and in-situ stress parameters of carbonate reservoirs using array sonic logging: A case study of Shunbei No.4 block

Abstract: [Objective] Geomechanical analysis plays a crucial role in exploring and developing oil and gas reservoirs. However, the study of in-situ stress in the Yijianfang–Yingshan formations of the Middle to Lower Ordovician in the Shunbei oilfield has lagged behind. This paper compares and analyzes the rock mechanics and in-situ stress characteristics of different types of carbonate reservoirs in the Yijianfang–Yingshan formations of the Lower Paleozoic Ordovician in the Shunbei No. 4 block, and explores the control effect of micro-grain structures on the in-situ stress and rock mechanics parameters of carbonate reservoirs. It aims to provide fundamental geological data for the evaluating of ultra-deep carbonate reservoirs in the Shunbei area. [Methods] This study, based on the spring combination model, determined the rock mechanics and in-situ stress characteristics through rock mechanics experiments and array acoustic logging, and characterized the micro-pore structure of the limestone using casting thin sections and X-ray μ -computed tomography analysis. [Results] The results indicate that the Young's modulus of the Yijianfang–Yingshan formations ranges from 50 to 89 GPa, the compressive strength from 99 to 136 MPa, and the Poisson's ratio from 0.25 to 0.32. The maximum horizontal principal stress of the formations ranges from 200 to 225 MPa, while the minimum horizontal principal stress ranges from 125 to 160 MPa. [Conclusion] Significant differences in rock mechanics parameters and in-situ stress exist among different types of carbonate reservoirs in the Yijianfang–Yingshan formations. From Type I to Type III and non-reservoir carbonate rocks, the Young's modulus, compressive strength, and maximum horizontal principal stress increase dramatically, while the Poisson's ratio and minimum horizontal principal stress show little change. Compared to micritic limestone, sandy–bioclastic limestone has larger calcite particles and reduced particle cohesion, resulting in decreased compressive strength and Young's modulus. Some calcite particles appear sub-rounded or rounded with higher three-dimensional particle sphericity, also leading to weaker intergranular engagement and further reduction in compressive strength and Young's modulus. The presence of numerous pores and fractures in sandy-bioclastic limestone facilitates frictional sliding and potential failure along microfractures or particle interfaces, contributing to lower compressive strength and Young's modulus as well. In addition, micritic limestones in the Yijianfang–Yingshan formations are affected by

基金项目: 中国博士后科学基金项目 (2018M631541); 中国地质调查局地质调查项目 (DD20221660-1, DD20242777)

This research is financially supported by the Chinese Postdoctoral Science Research Fund (Grant No. 2018M631541) and the Geological Survey Projects of the China Geological Survey (Grants No. DD20221660-1 and DD20242777).

第一作者: 刘军 (1982—), 男, 副研究员, 主要从事石油物探研究。Email: 408843381@qq.com

通讯作者: 周磊 (1987—), 男, 助理研究员, 主要从事石油地质研究。Email: zhoulei4010@126.com

收稿日期: 2023-06-28; 修回日期: 2023-09-22; 录用日期: 2023-09-22; 网络出版日期: 2023-09-22; 责任编辑: 范二平

hydrothermal activity, with some dolomite being replaced by quartz, which increases the compressive strength and Young's modulus. The macroscopic mechanical characteristics and rock mechanics parameters of the rock are constrained by the micro-grain structures. The low-value zones of the Young's modulus, compressive strength, and maximum horizontal principal stress in the Yijianfang–Yingshan formations are identified as the advantageous reservoir development zones in the Shunbei No. 4 block.

Keywords: Shunbei No. 4 block; carbonate rock; rock mechanic parameters; in-situ stress

摘要:地质力学分析在油气藏勘探开发过程中发挥着重要作用,顺北油气田中一下奥陶统一间房组—鹰山组储层地应力研究相对滞后。对比分析了顺北4号带下古生界中一下奥陶统一间房组—鹰山组碳酸盐岩不同类型储层的岩石力学和地应力特征,同时探讨了微观颗粒结构对碳酸盐岩储层地应力和岩石力学参数的控制作用,为顺北地区超深层碳酸盐岩储层评价提供了基础地质依据。基于弹簧组合模型,通过岩石力学实验和阵列声波测井确定了岩石力学和地应力特征,通过铸体薄片和X射线CT扫描表征碳酸盐岩的微观孔隙结构。研究表明:顺北4号带一间房组—鹰山组杨氏模量分布在50~89 GPa,抗压强度在99~136 MPa,泊松比在0.25~0.32;地层最大水平主应力为200~225 MPa,最小水平主应力为125~160 MPa。一间房组—鹰山组碳酸盐岩不同类型储层的岩石力学参数和地应力存在明显差异,从I类、II类、III类到非储层段碳酸盐岩的杨氏模量、抗压强度和最大水平主应力明显增大,而泊松比和最小水平主应力变化不大。相比于一间房组—鹰山组泥晶灰岩,砂屑-生屑灰岩方解石颗粒较大,颗粒黏结程度降低,导致岩石抗压强度和杨氏模量减小;砂屑-生屑灰岩部分方解石颗粒呈次圆状或圆状,颗粒三维空间球度较大,颗粒之间咬合作用减弱,使得岩石的抗压强度和杨氏模量减小;砂屑-生屑灰岩存在大量的孔隙和裂缝,灰岩易沿着潜在的微裂缝面或者颗粒接触面摩擦滑动甚至破裂,同样导致岩石抗压强度和杨氏模量减小。此外,一间房组—鹰山组泥晶灰岩受热液作用影响,部分白云石交代为石英,导致泥晶灰岩的抗压强度和杨氏模量增加。岩石的宏观力学特征和岩石力学参数受岩石微观颗粒结构的制约,一间房组—鹰山组杨氏模量、抗压强度和最大水平主应力低值区即为顺北4号带优势储层发育区带。

关键词: 顺北4号带;碳酸盐岩;岩石力学参数;地应力

中图分类号: P634.1 **文献标识码:** A **文章编号:** 1006-6616 (2024) 03-0394-14

DOI: 10.12090/j.issn.1006-6616.2023110

0 引言

顺北油气田位于顺托果勒低隆起,随着碳酸盐岩油藏勘探和开发技术的进步,在顺北超深层已经取得了重大油气突破(赵锐等,2019;漆立新,2020)。中一下奥陶统一间房组—鹰山组油气资源潜力巨大,国内诸多学者对顺北油气田断溶储集体的成因、分布和成藏进行了大量研究(焦方正,2018;张煜等,2023)。在中一下奥陶统鹰山组沉积期,大规模海侵导致海平面相对上升,顺北地区发育酸盐岩局限台地、开阔台地相沉积(王文博等,2021;赵永强,2022);在中奥陶统一间房组沉积期,受构造抬升影响,海平面相对下降,顺北地区发育台内礁滩相沉积(宋倩等,2016)。受台地相、台内礁滩相沉积环境影响,中一下奥陶统一间房组—鹰山组岩性组合以低能环境的泥—粉晶灰岩、细—粉晶白云岩、白云质灰岩为主,夹高能环境的砂屑灰

岩、砾屑灰岩、生物碎屑(生屑)灰岩和鲕粒灰岩。受多期构造改造、岩溶作用以及热液侵蚀影响,一间房组—鹰山组碳酸盐岩形成了高产能断溶型储集体(鲁新便等,2015),而断溶型储集体储层非均质性强、剩余油模式多样(柳州等,2014;朱秀香等,2023)。基于断裂几何学、运动学和动力学构造解析,确定顺北油田深部走滑断裂具有不同构造样式和“纵向分层、平面分段”的特征,提出走滑断裂控制油气在断裂不同部位的差异富集(邓尚等,2018;刘宝增,2020;陈平等,2023)。另外,通过方解石脉和流体包裹体分析,厘定了顺北油气田油气充注期次(王斌等,2020;韩强等,2021;宋刚等,2022;刘建章等,2023;漆立新和丁勇,2023;王玉伟等,2023),断裂既作为油气运移充注通道,又可成为油气的储集载体(金峰等,2023;王昱翔等,2023)。

地应力和岩石力学参数是控制储层裂缝发育的主要外因和内因,岩石中裂缝有利于改善储层孔隙度和渗透率(张贵生,2005;曾联波等,2007;丁文

龙等, 2015; 贾焰然等, 2021; 赵进雍等, 2022; 高晨阳等, 2023; 宋战平等, 2023)。孙东生等(2018)曾对比分析了不同地应力测量方法的差异性, 并计算和分析了顺南地区深层地应力大小、方向和应力环境。胡广强等(2017)指出顺北油田奥陶系桑塔木组辉绿岩弱理面效应可导致井壁失稳坍塌, 估算出辉绿岩层段的地应力和井壁坍塌压力。顺北油田一间房一鹰山组断溶储集体受走滑断裂影响易形成地层破碎带, 水平应力差极大(侯龙飞等, 2020; 张亚云等, 2022; 王伟吉等, 2022)。目前顺北地区有关岩石力学和地应力的研究主要集中在钻井井壁的稳定性, 而对顺北地区一间房组一鹰山组储层的岩石力学和地应力研究相对滞后, 从而制约了对碳酸盐岩储层的评价和认识。岩石的宏观力学特征和岩石力学参数的差异性主要受岩石微观颗粒结构的制约 (Přikryl, 2001; Potyondy and Cundall, 2004; Lindqvist et al., 2007; 马秋峰等, 2019; 刘圣鑫等, 2019), 岩石颗粒微观结构涉及颗粒大小 (Wong et al., 1996; Israeli and Emmanuel, 2018; Zhao et al., 2018; 韩振华等, 2019; 郭禹希等, 2022; 赵宁等, 2022)、颗粒形状 (Kock and Huhn, 2007; 孔亮和彭仁, 2011; 刘广等, 2013; 李树博等, 2019)、颗粒接触关系 (Billaux

et al., 2004; 蒋明镜等, 2013; 叶功勤等, 2019)、颗粒矿物成分、胶结物以及孔隙结构 (Kumar et al., 2012; Eliyahu et al., 2015; 刘圣鑫等, 2018)。因此, 文中通过岩芯 CT 扫描实验、三轴岩石力学实验和声发射实验, 结合阵列声波测井、地破实验以及钻井液漏失资料, 确定顺北 4 号带下古生界中一下奥陶统一间房组一鹰山组碳酸盐岩不同类型储层的岩石力学和地应力特征, 探讨微观颗粒结构对碳酸盐岩储层的地应力和岩石力学参数的控制作用, 为顺北地区超深层碳酸盐岩储层评价提供基础地质依据。

1 实验和方法

1.1 岩石力学实验

(1) 静态三轴岩石力学实验

岩芯来自 SHB41X 井、SHB42X 井、SHB43X 井、SHB44X 井(图 1), 采样深度在 7410~7630 m。钻取柱塞样, 岩芯两端磨平, 制成岩芯柱塞 2.5 cm×5.0 cm。依据三轴岩石力学实验方法 (GB/T 50266—2013), 将柱塞两端胶装密封后置于三轴试验机的高压釜, 围压分别设置为 0 MPa、25 MPa、50 MPa 和 75 MPa, 不同围压到达稳定后加载轴向载

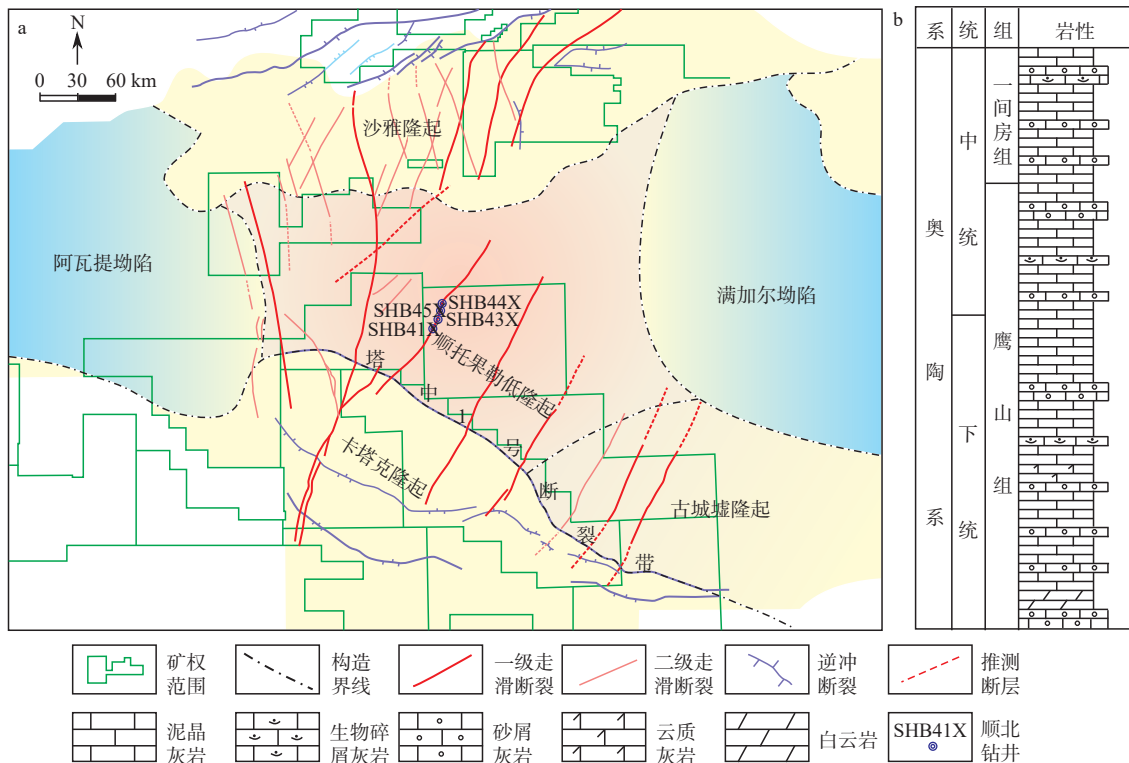


图 1 塔里木盆地顺北油气田构造位置和奥陶系储层岩性特征 (漆立新, 2020)

Fig. 1 Location of the Shunbei oil and gas field in the Tarim Basin (modified from Qi, 2020) and the lithological characteristics of the Ordovician reservoir

荷,直至一间房组一鹰山组碳酸盐岩柱塞破坏。建立一间房组一鹰山组碳酸盐岩样品不同围压下应力-应变曲线,计算获取静态岩石力学参数(表 1)。

表 1 动、静态岩石力学参数

Table 1 The dynamic and static rock mechanics parameters from geomechanical experiments

井号	井深/m	E_s /GPa	ν_s	E_d /GPa	ν_d	σ_h /MPa	σ_H /MPa
SHB41X	7543.30	52	0.222	72.24	0.342		
	7543.18	58	0.287	75.04	0.312	147	200
SHB43X	7570.05	62	0.267	79.53	0.32	143	213
	7570.25	64	0.239	79.73	0.346		
SHB43X	7572.24	63	0.291	79.51	0.317		
SHB44X	7632.79	57	0.270	79.67	0.304	149	212
SHB44X	7634.66	45	0.298	71.44	0.302		

注: E_s —静态杨氏模量, GPa; ν_s —静态泊松比, 无量纲; E_d —动态杨氏模量, GPa; ν_d —动态泊松比, 无量纲; σ_h —最小水平主应力, MPa; σ_H —最大水平主应力, MPa

(2) 声发射实验

取岩芯柱塞样(2.5 cm×5.0 cm),将两端胶装的碳酸盐岩柱塞三轴压力加载,声波发射测试系统检测信号,记录声发射的撞击、幅值、峰值和信号强度等参数,基于识别 Kaiser 效应信号,获取一间房组一鹰山组碳酸盐岩样品的最大、最小水平主应力(表 1)。

(3) CT 扫描实验

取岩芯柱塞样(2.5 cm×5.0 cm)置于 Zeiss X Radia 510 Versa 高分辨率三维 X 射线显微镜。CT 扫描使用加速电压为 60 kV、功率为 5 W 的 X 射线,源距、目距和曝光时间分别设置为 8.0 mm、69.4 mm 和 3 s。显微照片的像素大小达到 0.7 μm,Dragonfly 软件对 CT 扫描数据集进行解释。

1.2 岩石力学参数和地应力计算方法

(1) 动态岩石力学参数

一间房组一鹰山组地层纵、横波速度均可由全井段阵列声波测井获得,结合横、纵波速度和密度测井曲线,确定一间房组一鹰山组动态岩石力学参数:

$$E_d = \frac{\rho V_s^2 (3V_p^2 - 4V_s^2)}{V_p^2 - V_s^2} \quad (1)$$

$$\nu_d = \frac{V_p^2 - 2V_s^2}{2(V_p^2 - V_s^2)} \quad (2)$$

式中, E_d —动态杨氏模量, GPa; ν_d —动态泊松比; V_p —横波速度, m/s; V_s —纵波速度, m/s; ρ —岩石

密度, g/cm³。

(2) 垂向应力

垂向应力是上覆在目的层位的地层岩石和岩层孔隙中滞留流体的总重力,一间房组一鹰山组地层垂向应力可由密度测井数据根据井深积分求得:

$$\sigma_v = \int_0^z \rho_z g dz \quad (3)$$

式中, σ_v —垂向应力, MPa; z —地层深度, m; ρ_z — z 深度的岩石密度, g/cm³; g 为重力加速度,取值为 9.807m/s²。

(3) 地层压力

顺北 4 号带一间房组一鹰山组为台地相沉积,地层岩性组合中泥岩欠发育,不能采用泥岩正常压实理论,因此地层压力计算采用 Bowers 法(Bowers, 1995)计算地层压力模型:

$$p_p = \sigma_v - \left(\frac{V_s - 1500}{A} \right)^{\frac{1}{B}} \quad (4)$$

其中, p_p —地层压力, MPa; σ_v —垂向应力, MPa; V_s —纵波速度, m/s; A 、 B —地区经验参数,无量纲。

(4) 水平地应力

相比于葛氏模型、黄氏模型和单轴应变模型,弹簧组合模型考虑垂向应力、非均匀分布的构造应力和岩层强度对水平应力影响(黄荣樽等, 1993; Walls and Dvorkin, 1994; 葛洪魁等, 1998; 印兴耀等, 2018)。Wu(2001)指出 Biot 系数(α)会随着孔隙度增大而增加,建立了 Biot 系数和孔隙度模型。在确

定的地层压力、垂向应力和岩石力学参数前提下,采用弹簧组合模型计算顺北4号带一间房组一鹰山组的水平地应力:

$$\sigma_h = \frac{\nu}{1-\nu}\sigma_v + \frac{1-2\nu}{1-\nu}\alpha p_p + \frac{E\varepsilon_h}{1-\nu^2} + \frac{\nu E\varepsilon_H}{1-\nu^2} \quad (5)$$

$$\sigma_H = \frac{\nu}{1-\nu}\sigma_v + \frac{1-2\nu}{1-\nu}\alpha p_p + \frac{E\varepsilon_H}{1-\nu^2} + \frac{\nu E\varepsilon_h}{1-\nu^2} \quad (6)$$

式中, σ_h 、 σ_H —最小水平主应力、最大水平主应力, MPa; α —Biot系数, 无量纲; E —杨氏模量, MPa; ν —泊松比, 无量纲; ε_H 、 ε_h —岩层在最大和最小水平应力方向的应变, 无量纲; 其他变量同上。

2 实验结果

2.1 动、静态岩石力学参数

基于岩芯三轴岩石力学实验的应力-应变曲线, 估算了顺北4号带一间房组一鹰山组碳酸盐岩储层段的静态杨氏模量和静态泊松比(表1)。一间房组一鹰山组灰岩的静态杨氏模量为45~64 GPa, 平均为57 GPa; 静态泊松比为0.222~0.298, 平均为0.268。基于阵列声波的横波速度、纵波速度和密度

测井, 依据公式(3)和(4), 确定一间房组一鹰山组碳酸盐岩全井段的动态杨氏模量和泊松比。一间房组一鹰山组灰岩的动态杨氏模量为71.44~79.73 GPa, 平均为76.73 GPa; 动态泊松比为0.302~0.346, 平均为0.32。顺北4号带一间房组一鹰山组地层遭受多期表生岩溶和热液岩溶作用(鲁新便等, 2015; 伍齐乔等, 2019; 宋刚等, 2022), 碳酸盐岩储层含有微裂隙和溶蚀缝/洞(柳洲等, 2014; 卜旭强等, 2023), 碳酸盐岩储层内部缝、洞系统导致动态和静态岩石力学参数的差异。国内外诸多学者提出动、静态岩石力学参数校正模型, 动、静态岩石力学参数常呈现线性或二项式关系(Ezati et al., 2020; 郭思强, 2020; 舒红林等, 2021)。顺北4号带灰岩动、静态岩石力学参数拟合呈良好的线性关系(图2)。基于动、静态杨氏模量和泊松比线性关系($E_s=1.6765E_d-71.36$; $\nu_s=-1.4122\nu_d+0.7201$), 将基于测井数据计算的动态杨氏模量和泊松比转为静态杨氏模量和泊松比, 计算一间房组一鹰山组全井段静态杨氏模量和泊松比。

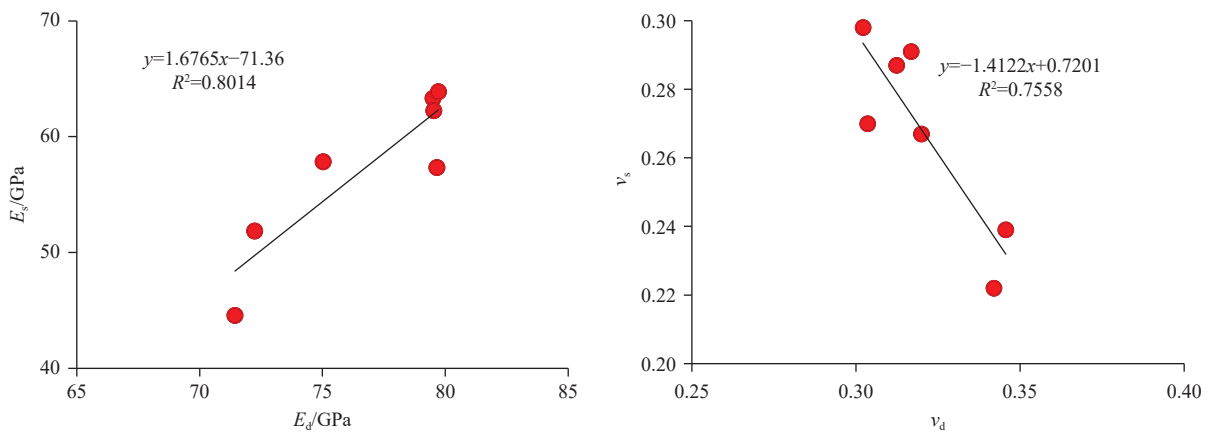


图2 动、静态岩石力学参数关系图

Fig. 2 The correlations between dynamic and static rock mechanics parameters

2.2 地应力

基于声发射实验的Kaiser效应, 顺北4号带一间房组一鹰山组灰岩的最大水平主应力为200~213 MPa, 最小水平主应力为143~149 MPa(表1)。结合现场静水压力测试(表2), 通过最小二乘法拟合估算Bowers法A和B 2个待定系数分别为4.45和1.53。结合声发射实验计算地应力和钻井现场地破实验数据(表2), 通过最小二乘法拟合估算

ε_H 和 ε_h 2个待定系数分别为0.00118和-0.000177。基于弹簧组合模型, 依据公式(7)和(8), 确定一间房组一鹰山组碳酸盐岩最大水平主应力和最小水平主应力, 建立顺北4号带SB41X井、SB42X井、SB43X井和SB44X井的地应力剖面。顺北4号带一间房组一鹰山组杨氏模量为50~89 GPa, 抗压强度为99~136 MPa, 泊松比为0.25~0.32。顺北4号带一间房组一鹰山组最大水平主应力为170~230

表2 顺北4号带地破实验参数和地层压力

Table 2 The LOT parameters and formation pressure for the Shunbei No. 4 block

井名	地破层位	地破深度/m	地破当量密度/(g/cm ³)	地破压力	深度/m	地层压力/MPa
SHB41X	库车组	1500	1.97	29.0	7500	90.67
	卡拉沙依组	4349	1.55	66.1	7984	92.51
SHB42X	吉迪克组	2009	1.96	38.6		
	却尔却克组	6140	1.74	104.7		
SHB43X	库车组	1505	1.84	27.1	2500	64.21
	卡拉沙依组	4441	1.55	67.5	7944	91.97
SHB44X	库车组	1509	2.18	32.2	7431	88.44
	卡拉沙依组	4430	1.72	74.7	7882	90.55

MPa, 最小水平主应力为 125~160 MPa。

2.3 不同类型储层的岩石力学参数和地应力特征

基于碳酸盐岩储层类型划分和测井解释, 顺北4号带一间房组一鹰山组碳酸盐岩可划分为4类: I类洞穴型储层、II类裂缝-孔洞型储层、III类溶蚀孔洞型储层和非储层(傅海成等, 2006; 马乃拜等, 2019; 马永生等, 2019; 吕海涛等, 2021; 宁超众等, 2021; 陈雨霖和唐军, 2022; 史江涛等, 2022)。针对一间房组一鹰山组碳酸盐岩不同类型的储层, 开展了其岩石力学和地应力参数分析对比(图3, 图4)。I类洞穴型储层杨氏模量集中在45~65 GPa, 频数峰值为55 GPa; II类裂缝-孔洞型储层杨氏模量集中在55~70 GPa, 频数峰值为60 GPa; III类孔洞型储层杨氏模量集中在65~85 GPa, 频数峰值为80 GPa; 非储层杨氏模量集中在70~90 GPa, 峰值为85 GPa。顺北地区一间房组一鹰山组从I类、II类、III类储层到非储层, 岩石杨氏模量和抗压强度逐渐增大, 泊松比差异不明显。I类洞穴型储层最大水平主应力集中在170~210 MPa, 频数峰值为180 MPa; II类裂缝-孔洞型储层最大水平主应力集中在180~210 MPa, 频数峰值为190 MPa; III类孔洞型储层最大水平主应力集中在190~220 MPa, 频数峰值为200 MPa; 非储层最大水平主应力集中在200~230 MPa, 频数峰值为210 MPa。不同储层地应力参数对比如图4所示, 频数主峰明显右移, 表明顺北地区一间房组一鹰山组从I类、II类、III类储层到非储层, 最大水平主应力和水平应力差逐渐增大。

3 讨论

基于阵列声波测井估算一间房组一鹰山组全井段砂屑-生屑灰岩和泥晶灰岩的地应力和岩石力学参数(图5), 非储层段泥晶灰岩层段的抗压强度、杨氏模量、最大水平主应力和最小水平主应力远大于储层段的砂屑-生屑灰岩。一间房组一鹰山组非储层段泥晶灰岩含少量介形虫、腕足生物碎屑, 方解石晶粒小, 主要由泥晶-微晶方解石构成, 泥晶灰岩受深部热液影响, 石英局部交代方解石(焦方正, 2018; 马乃拜等, 2019; 马永生等, 2019; 伍齐乔等, 2019), 石英呈自形、半自形(图6a、6b)。一间房组一鹰山组储层段砂屑-生屑灰岩富含生物碎屑(尚凯等, 2017; 宋倩等, 2018), 方解石晶粒较大, 粒屑结构清晰, 部分储层段的方解石颗粒呈次圆状或椭圆状(图6c、6d)。

泥晶灰岩方解石晶粒粒径小, 晶粒与晶粒接触面积增加, 晶粒黏结程度增大; 砂屑-生屑灰岩方解石粒径较大, 颗粒之间通过泥晶-微晶方解石胶结, 颗粒黏结程度降低。Johansson(2011)指出岩石颗粒大小影响岩石力学性质, 随着岩石颗粒粒径的减小, 岩石抗压强度和杨氏模量逐渐增加(Wong et al., 1996; 康瀚, 2013; 陈绍杰等, 2017; Zhao et al., 2018; 韩振华等, 2019; 赵宁等, 2022)。泥晶灰岩方解石晶粒不规则, 晶粒棱角分明, 颗粒之间咬合作用大; 砂屑-生屑灰岩岩石颗粒呈次圆状或圆状, 颗粒三维空间球度较大, 颗粒之间咬合作用减弱。岩石颗粒形状对其宏观力学存在影响(Kock and Huhn,

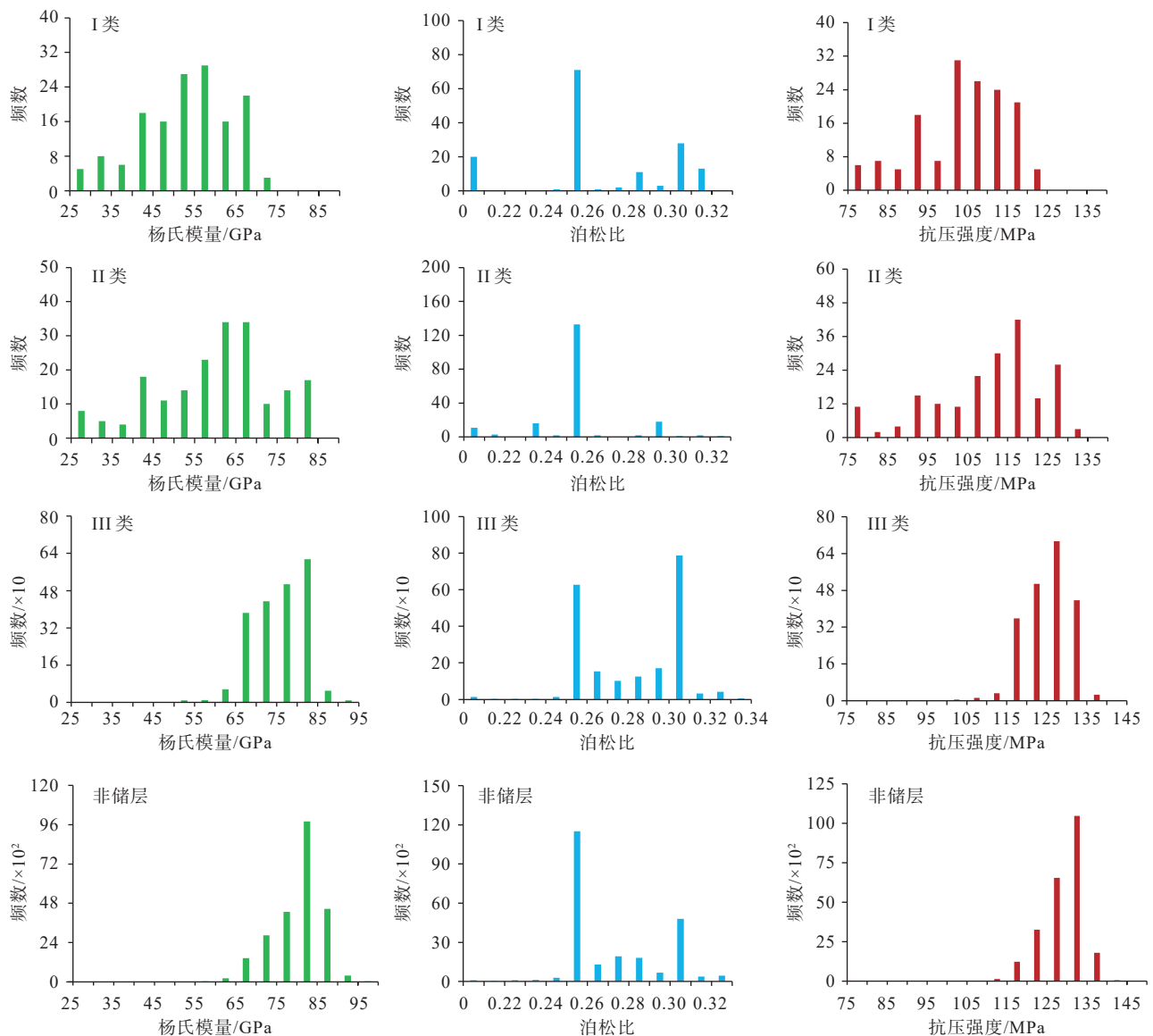


图3 不同类型储层的岩石力学参数对比图

Fig. 3 The comparison charts of rock mechanics parameters for different types of reservoirs

2007; 刘广等, 2013; 李树博等, 2019), 随着岩石/矿物颗粒球度逐渐减小, 岩石的抗压强度和杨氏模量逐渐增大(Shinohara et al., 2000; Dodds, 2003)。

岩石宏观力学特征和地力学参数除了受岩石微观结构如颗粒大小、颗粒形状和颗粒接触关系的影响外, 还会受到岩石颗粒的矿物成分和孔隙结构制约(Kumar et al., 2012; Eliyahu et al., 2015; 刘圣鑫等, 2018)。一间房组一鹰山组台地相灰岩经历了多期岩溶和热液岩溶改造, 特别是加里东早期和海西晚期的热液作用(焦方正, 2018; 马永生等, 2019; 伍齐乔等, 2019), 泥晶白云石、方解石重结晶并交代为中—巨晶白云石、方解石和石英(图 6a、6b)。岩石中不同矿物组分的微观岩石力学性质存在差

异(Kumar et al., 2012; Eliyahu et al., 2015; 刘圣鑫等, 2018), 一间房组一鹰山组泥晶灰岩交代产生的石英导致非储层段泥晶灰岩的抗压强度和杨氏模量增加。对比分析 III 类储层和非储层段的岩石 CT 成像发现, 非储层段灰岩致密, 不发育微裂缝和孔隙(图 7a、7b), III 类储层发育多条微裂缝(图 7c、7d)。一间房组一鹰山组碳酸盐岩优质储层内部存在大量的孔隙、裂缝或者洞穴, 外力作用可导致岩石孔隙结构变形, 储层段灰岩沿着潜在的微裂缝面或者颗粒接触面摩擦滑动甚至破裂(葛洪魁等, 2001; 赵宁等, 2022)。含微裂隙储层段砂屑灰岩在受到外力作用时, 颗粒层面滑动和破裂使得轴向应变增量变大, 导致岩石的抗压强度和杨氏模量减小

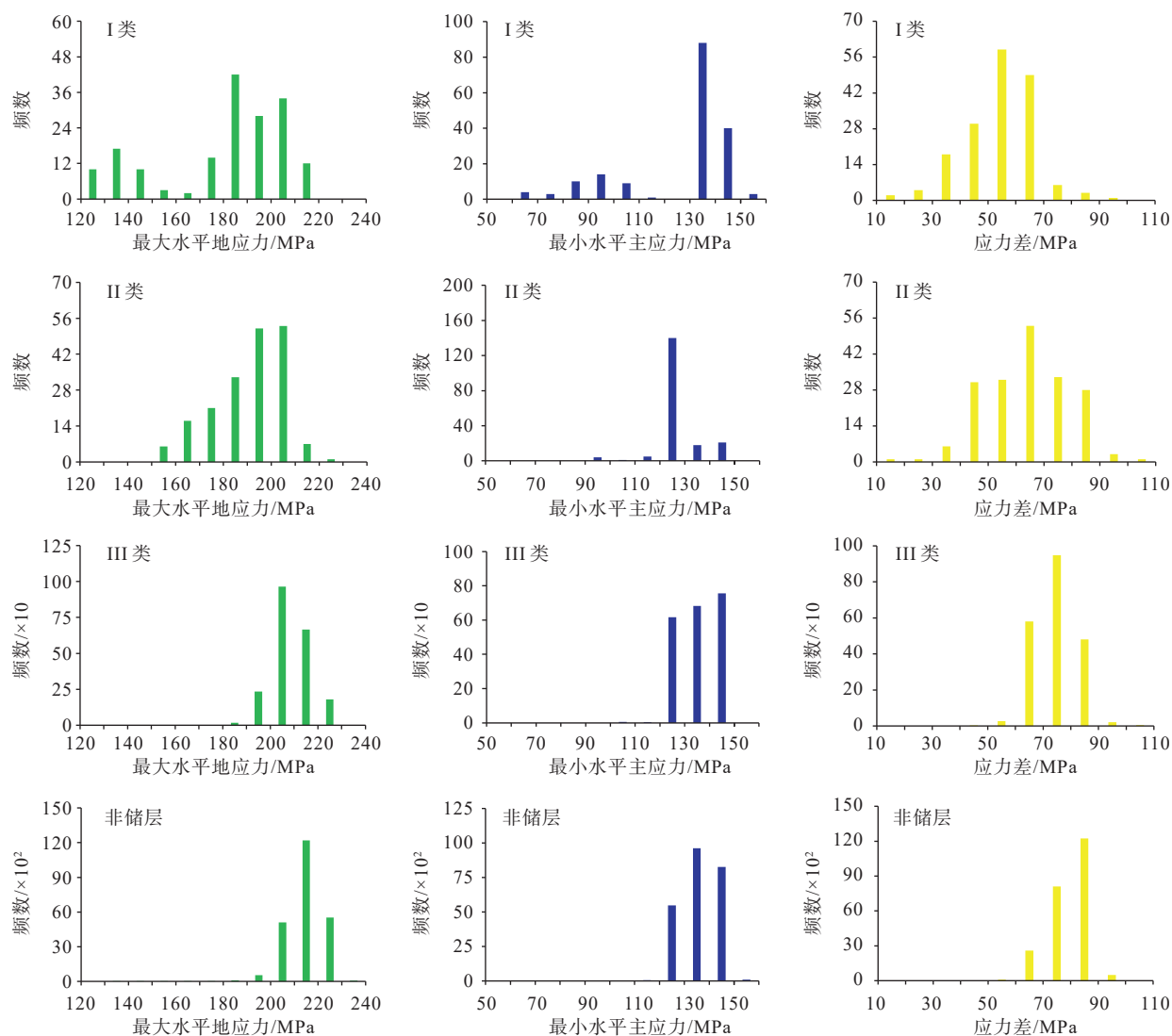


图4 不同类型储层的地应力参数对比图

Fig. 4 The comparison charts of in-situ stress parameters for different types of reservoirs

(李智武等, 2005; 刘荣和等, 2008; 夏在连等, 2008; 杨海博和武云云, 2011; 杨琦等, 2017)。

以SHB43X井地破实验和室内声发射实验获取的地应力参数为例,库车组(1505 m井段)和卡拉沙依组(4441 m井段)的地破压力为27.1 MPa和67.5 MPa(表2),鹰山组(7570.05 m井段)室内测得的最小水平主应力和最大水平主应力分别为143 MPa和213 MPa。基于阵列声波测井估算库车组(1505 m井段)和卡拉沙依组(4441 m井段)的最小水平主应力为25.6 MPa和65.7 MPa;鹰山组(7570.05 m井段)的最小水平主应力和最大水平主应力分别为139 MPa和209.7 MPa。对比3种方法得到的地应力可知,基于阵列声波测井估算地应力误差在1.8%~5.6%,具有合理精度。综上所述,相比于一间房组—鹰山组

非储层灰岩,储层段灰岩的杨氏模量减小,形成层内相对“软弱层段”,而非储层灰岩成为相对“能干层段”,导致储层段灰岩水平最大地应力和应力差减小。

4 结论

(1)顺北4号带一间房组—鹰山组碳酸盐岩的杨氏模量为50~89 GPa,抗压强度为99~136 MPa,泊松比为0.25~0.32;其最大水平主应力为200~225 MPa,最小水平主应力为125~160 MPa。

(2)顺北4号带一间房组—鹰山组碳酸盐岩可划分为4类:I类洞穴型储层、II类裂缝-孔洞型储层、III类溶蚀孔洞型储层和非储层,其中I类洞穴

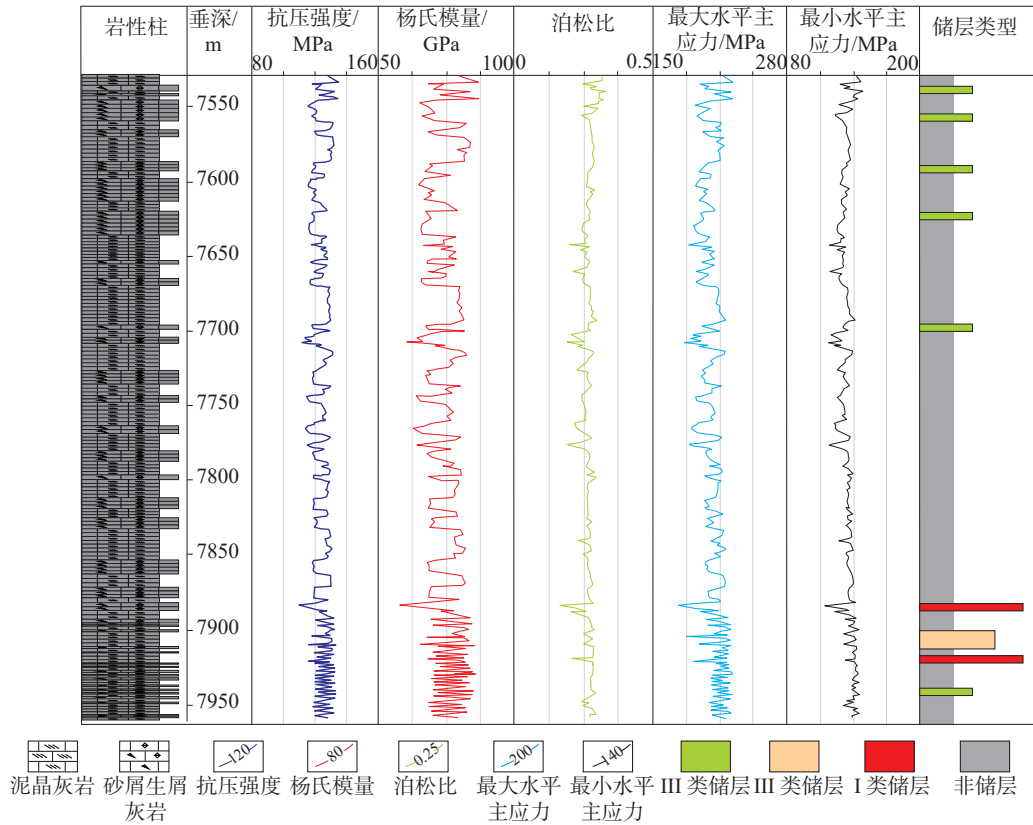
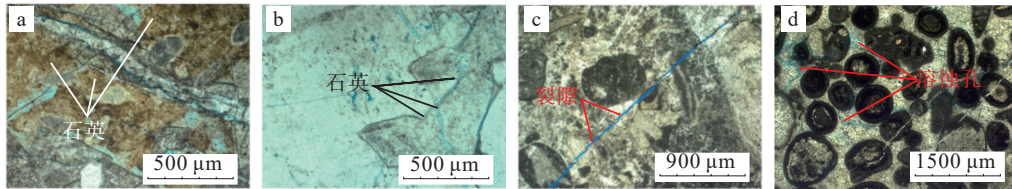


图 5 SHB41X 井地应力和岩石力学参数剖面

Fig. 5 The profile of in-situ stress and rock mechanics parameters for well SHB41X

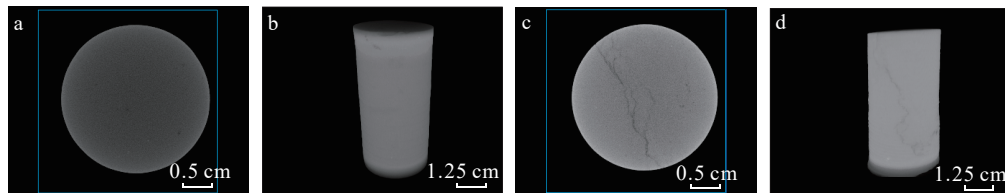


a—含硅质泥晶灰岩, SHB45X 井 7722 m; b—泥晶灰岩, SHB45X 井 7724 m; c—生屑灰岩, SHB45X 井 7725 m; d—鲕粒灰岩, SHB45X 井 7727 m

图 6 SHB45X 井一间房组灰岩类型

Fig. 6 Limestone types of the Yijianfang Formation in well SHB45

(a) Siliceous micritic limestone, at 7722 m in well SHB45X; (b) Micritic limestone, at 7724 m in well SHB45X; (c) Bioclastic limestone, at 7725 m in well SHB45X; (d) Oolitic limestone, at 7727 m in well SHB45X



a—非储层段灰岩 CT 切片, SHB43X 井 7570.25 m; b—非储层段灰岩柱塞 CT 成像, SHB43X 井 7570.25 m; c—III类储层灰岩 CT 切片 SHB41X 井, 7543.3 m; d—III类储层灰岩柱塞 CT 成像, SHB41X 井 7543.3 m

图 7 不同类型储层裂缝 CT 成像

Fig. 7 CT images of fractures in different reservoirs

(a) CT slice of limestone in the non-reservoir section, at 7570.25 m in well SHB43X; (b) CT image of limestone plug in the non-reservoir section, at 7570.25 m in well SHB43X; (c) CT slice of limestone in Type III reservoir, at 7543.3 m in well SHB41X; (d) CT image of limestone plug in Type III reservoir, at 7543.3 m in well SHB41X

型储层杨氏模量集中在45~65 GPa,最大水平主应力集中在170~210 MPa; II类裂缝-孔洞型储层杨氏模量集中在55~70 GPa,最大水平主应力集中在180~210 MPa; III类孔洞型储层杨氏模量集中在65~85 GPa,最大水平主应力集中在190~220 MPa;非储层段杨氏模量集中在70~90 GPa,最大水平主应力集中在200~230 MPa;一间房组-鹰山组碳酸盐岩不同类型储层的岩石力学参数和地应力存在明显差异,从I类、II类、III类储层到非储层段碳酸盐岩的杨氏模量、抗压强度和最大水平主应力明显增大。

(3)一间房组-鹰山组非储层段的泥晶灰岩和不同类型的储层砂屑-生屑灰岩的颗粒微观结构差异分析表明,砂屑-生屑灰岩中方解石晶粒大、呈扁圆状或次圆状,后期热液交代和构造微裂缝存在,因此I类、II类砂屑-生屑灰岩储层具有较低的抗压强度和杨氏模量以及最大水平主应力。

References

- BILLAUX D, DEDECKER F, CUNDALL P, 2004. A novel approach to studying rock damage: the three dimensional adaptive continuum/discontinuum code[J]. *Rock Engineering*, 723-728.
- Bowers G. L. . Pore pressure estimation from velocity data: accounting for overpressure mechanisms besides undercompaction[J]. *SPE Drilling & Completion*, 1995, 10(2): 89-95.
- BU X Q, WANG L Y, ZHU L H, et al, 2023. Characteristics and reservoir accumulation model of Ordovician fault-controlled fractured-vuggy reservoirs in Shunbei oil and gas field, Tarim Basin[J]. *Lithologic Reservoirs*, 35(3): 152-160. (in Chinese with English abstract)
- CHEN P, NENG Y, WU X, et al, 2023. Stratification and segmentation characteristics and tectonic evolution of Shunbei No. 5 strike-slip fault zone in Tarim Basin[J]. *Xinjiang Petroleum Geology*, 44(1): 33-42. (in Chinese with English abstract)
- CHEN S J, GUO Y H, HUANG W P, et al, 2017. Experimental study of influence regularity and mechanism of particle size on mechanical properties of red sandstone[J]. *Journal of Shandong University of Science and Technology (Natural Science)*, 36(6): 8-14. (in Chinese with English abstract)
- CHEN Y L, TANG J, 2022. Well logging evaluation of fractures and Vugs of carbonate reservoirs in Tuofutai area of Tarim Basin, Xinjiang, China[J]. *Chinese Journal of Engineering Geophysics*, 19(5): 689-698. (in Chinese with English abstract)
- DENG S, LI H L, ZHANG Z P, et al, 2018. Characteristics of differential activities in major strike-slip fault zones and their control on hydrocarbon enrichment in Shunbei area and its surroundings, Tarim Basin[J]. *Oil & Gas Geology*, 39(5): 878-888. (in Chinese with English abstract)
- DING W L, YIN S, WANG X H, et al, 2015. Assessment method and characterization of tight sandstone gas reservoir fractures[J]. *Earth Science Frontiers*, 22(4): 173-187. (in Chinese with English abstract)
- DODDS J S, 2003. Particle shape and stiffness: effects on soil behavior[D]. Atlanta: Georgia Institute of Technology.
- ELIYAHU M, EMMANUEL S, DAY-STIRRAT R J, et al, 2015. Mechanical properties of organic matter in shales mapped at the nanometer scale[J]. *Marine and Petroleum Geology*, 59: 294-304.
- EZATI M, AZIZADEH M, RIAHI M A, et al, 2020. Wellbore stability analysis using integrated geomechanical modeling: a case study from the Sarvak reservoir in one of the SW Iranian oil fields[J]. *Arabian Journal of Geosciences*, 13(4): 149.
- FU H C, ZHANG C S, ZHAO L X, et al, 2006. Identification of the reservoir space types of the carbonate reservoir in Lunnan area of Tarim Basin by means of logging data[J]. *Journal of Xi'an Shiyou University (Natural Science Edition)*, 21(5): 38-41. (in Chinese with English abstract)
- GAO C Y, ZHAO F H, GAO L F, et al, 2023. The methods of fracture prediction based on structural strain analysis and its application[J]. *Journal of Geomechanics*, 29(1): 21-33. (in Chinese with English abstract)
- GB/T 50266—2013. 2013. Standard for testing methods for engineering rock masses[S]. Beijing, China Planning Press.(in Chinese)
- GE H K, LIN Y S, WANG S C, 1998. In situ stresses determination technique and its applications in petroleum exploration and development[J]. *Journal of the University of Petroleum (Edition of Natural Science)*, 22(1): 94-99. (in Chinese with English abstract)
- GE H K, CHEN Y, LIN Y S, 2001. Microscopic mechanism of difference between static and dynamic elastic parameters of rock[J]. *Journal of China University of Petroleum (Edition of Natural Science)*, 25(4): 34-36. (in Chinese with English abstract)
- GUO S Q, 2020. Rock mechanical parameter modeling of Fuyu tight oil reservoir in Well Block T30 of Daqing Oilfield[J]. *Petroleum Geology & Oilfield Development in Daqing*, 39(5): 169-174. (in Chinese with English abstract)
- GUO Y X, QIN Y, WANG H, et al, 2022. Physical modelling of particle size on mechanical properties of broken rock[J]. *Science Technology and Engineering*, 22(11): 4489-4496. (in Chinese with English abstract)
- HAN Q, YUN L, JIANG H S, et al, 2021. Marine oil and gas filling and accumulation process in the north of Shuntuoguole area in northern Tarim basin[J]. *Journal of Jilin University (Earth Science Edition)*, 51(3): 645-658. (in Chinese with English abstract)
- HAN Z H, ZHANG L Q, ZHOU J, et al, 2019. Uniaxial compression test and numerical studies of grain size effect on mechanical properties of granite[J]. *Journal of Engineering Geology*, 27(3): 497-504. (in Chinese with English abstract)
- HOU L F, YANG C H, GUO Y T, et al, 2020. Simulation study on crack steering of near-wellbore in crack-hole type carbonate rock[J]. *Science Technology and Engineering*, 20(27): 11080-11086. (in Chinese with English abstract)
- HU G Q, BAI B Z, KE K, 2017. Analysis on borehole instability mechanism of diabase in Shunbei Block[J]. *China Offshore Oil and Gas*, 29(5): 119-125. (in Chinese with English abstract)
- HUANG R Z, BAI J Z, ZHOU Y H, et al, 1993. The relationship between the location and direction of tensile cracks on the wellbore wall of inclined

- vertical wells and wellbore pressure[J]. *Oil Drilling & Production Technology*, 15(5): 7-11. (in Chinese)
- ISRAELI Y, EMMANUEL S, 2018. Impact of grain size and rock composition on simulated rock weathering[J]. *Earth Surface Dynamics*, 6(2): 319-327.
- JIA Y R, SHI J T, LI X H, et al, 2021. Classification and evaluation methods for low-permeability tight gas wells in the Zizhou gas field of Changqing[J]. *Geology and Exploration*, 2021, 57(3): 647-655. (in Chinese with English abstract)
- JIANG M J, BAI R P, LIU J D, et al, 2013. Experimental study of inter-granular particles bonding behaviors for rock microstructure[J]. *Chinese Journal of Rock Mechanics and Engineering*, 32(6): 1121-1128. (in Chinese with English abstract)
- JIAO F Z, 2018. Significance and prospect of ultra-deep carbonate fault-karst reservoirs in Shunbei area, Tarim Basin[J]. *Oil & Gas Geology*, 39(2): 207-216. (in Chinese with English abstract)
- JIN F, ZHU X X, YU Y X, et al, 2023. Structural geometry and evolution of the No. 13 strike-slip fault zone in the Shunbei Area, Tarim Basin[J]. *Geotectonica et Metallogenia*, 47(1): 54-65. (in Chinese with English abstract)
- JOHANSSON E, 2011. Technological properties of rock aggregates[D]. Luleå: University of Technology.
- KANG H, 2013. Experimental study on mechanical characteristics of Triaxial compression of sandstone in different sizes[J]. *Subgrade Engineering*(6): 94-96, 101. (in Chinese with English abstract)
- KOCK I, HUH N K, 2007. Influence of particle shape on the frictional strength of sediments: A numerical case study[J]. *Sedimentary Geology*, 196(1-4): 217-233.
- KONG L, PENG R, 2011. Particle flow simulation of influence of particle shape on mechanical properties of quasi-sands[J]. *Chinese Journal of Rock Mechanics and Engineering*, 30(10): 2112-2119 (in Chinese with English abstract)
- KUMAR V, CURTIS M E, GUPTA N, et al , 2012. Estimation of elastic properties of organic matter and woodford shale through nano-indentation measurements[C]//Proceedings of SPE Canadian unconventional resources conference. Calgary, Canada: SPE.
- LI S B, JIANG W, ZHANG X G, et al, 2019. The main controlling factors and evolutionary sequence of Ordovician fracture in H gas field of Bachu uplift, Tarim Basin[J]. *Journal of Geomechanics*, 25(4): 518-526. (in Chinese with English abstract)
- LI Z W, LUO Y H, LIU S G, et al, 2005. The main controlling factors and evolutionary sequence of ordovician fracture in H gas field of Bachu uplift, Tarim basin[J]. *Journal of Mineralogy and Petrology*, 25(4): 52-60. (in Chinese with English abstract)
- LINDQVIST J E, ÅKESSON U, MALAGA K, 2007. Microstructure and functional properties of rock materials[J]. *Materials Characterization*, 58(11-12): 1183-1188.
- LIU B Z, 2020. Analysis of main controlling factors of oil and gas differential accumulation in Shunbei area, Tarim Basin - taking Shunbei No. 1 and No. 5 strike slip fault zones as examples[J]. *China Petroleum Exploration*, 25(3): 83-95. (in Chinese with English abstract)
- LIU G, RONG G, PENG J, et al, 2013. Mechanical behaviors of rock affected by mineral particle shapes[J]. *Chinese Journal of Geotechnical Engineering*, 35(3): 540-550. (in Chinese with English abstract)
- LIU J Z, CAI Z X, TENG C Y, et al, 2023. Coupling relationship between formation of calcite veins and hydrocarbon charging in Middle-Lower Ordovician reservoirs in strike-slip fault zones within craton in Shunbei area, Tarim Basin[J]. *Oil & Gas Geology*, 44(1): 125-137. (in Chinese with English abstract)
- LIU R H, FENG W G, LONG L, et al, 2008. Experimental studies on the mechanics and acoustics of tight carbonate rock[J]. *Petroleum Geology & Oilfield Development in Daqing*, 27(6): 131-135. (in Chinese with English abstract)
- LIU S X, WANG Z X, ZHANG L Y, et al, 2018. Micromechanics properties analysis of shale based on nano-indentation[J]. *Journal of Experimental Mechanics*, 33(6): 957-968. (in Chinese with English abstract)
- LIU S X, WANG Z X, ZHANG L Y, et al, 2019. Effects of microstructure characteristics of shale on development of complex fracture network[J]. *Journal of Mining and Safety Engineering*, 36(2): 420-428. (in Chinese with English abstract)
- LIU Z, KANG Z H, ZHOU L, et al, 2014. Distribution model of remaining oil of fractured-vuggy carbonate reservoir in 6-7 Area, Tahe Oilfield[J]. *Geoscience*, 28(2): 369-378. (in Chinese with English abstract)
- LU X B, HU W G, WANG Y, et al, 2015. Characteristics and development practice of fault-karst carbonate reservoirs in Tahe area, Tarim Basin[J]. *Oil & Gas Geology*, 36(3): 347-355. (in Chinese with English abstract)
- LÜ H T, HAN J, ZHANG J B, et al, 2021. Development characteristics and formation mechanism of ultra-deep carbonate fault-dissolution body in Shunbei area, Tarim Basin[J]. *Petroleum Geology & Experiment*, 43(1): 14-22. (in Chinese with English abstract)
- MA N B, MA X P, DU W W, et al, 2019. Developmental characteristics for the carbonate reservoir in Ordovician in first area of SHUNBEI[J]. *Inner Mongolia Petrochemical Industry*, 45(7): 106-112. (in Chinese)
- MA Q F, QIN Y P, ZHOU T B, et al, 2019. Constitutive model of rock compaction stage based on contact theory[J]. *Journal of Central South University (Science and Technology)*, 50(8): 1941-1948. (in Chinese with English abstract)
- MA Y S, HE Z L, ZHAO P R, et al, 2019. A new progress in formation mechanism of deep and ultra-deep carbonate reservoir[J]. *Acta Petrolei Sinica*, 40(12): 1415-1425. (in Chinese with English abstract)
- NING C Z, SUN L D, HU S Y, et al, 2021. Karst types and characteristics of the Ordovician fracture-cavity type carbonate reservoirs in Halahatang oilfield, Tarim Basin[J]. *Acta Petrolei Sinica*, 42(1): 15-32. (in Chinese with English abstract)
- POTYONDY D O, CUNDALL P A, 2004. A bonded-particle model for rock[J]. *International Journal of Rock Mechanics and Mining Sciences*, 41(8): 1329-1364.
- PRĪKRYL R, 2001. Some microstructural aspects of strength variation in rocks[J]. *International Journal of Rock Mechanics and Mining Sciences*, 38(5): 671-682.
- QI L X, 2020. Characteristics and inspiration of ultra-deep fault-karst reservoir in the Shunbei area of the Tarim Basin[J]. *China Petroleum Exploration*, 25(1): 102-111. (in Chinese with English abstract)
- QI L X, DING Y, 2023. Differences in marine hydrocarbon accumulation

- between the eastern and western parts of Shunbei area, Tarim Basin[J]. *Petroleum Geology & Experiment*, 45(1): 20-28. (in Chinese with English abstract)
- SHANG K, GUO N, CAO Z C, et al, 2017. Main controlling factors of reservoir in Ordovician Yijianfang Formation on the northern slope of Middle Tarim Basin[J]. *Marine Origin Petroleum Geology*, 22(1): 39-46. (in Chinese with English abstract)
- SHI J T, HAO J M, WANG X L, 2022. Reservoir characteristics and controlling factors of Lower-Middle Ordovician Yingshan Formation in Tahe area[J]. *Journal of Jilin University (Earth Science Edition)*, 52(2): 348-362. (in Chinese with English abstract)
- SHINOHARA K, OIDA M, GOLMAN B, 2000. Effect of particle shape on angle of internal friction by triaxial compression test[J]. *Powder Technology*, 107(1-2): 131-136.
- SHU H L, QIU K B, LI Q F, et al, 2021. A method for evaluating the geomechanical characteristics of shale gas: the geomechanical characteristics of the mountain shale in the intensively reworked marine area of South China[J]. *Natural Gas Industry*, 41(S1): 1-13. (in Chinese with English abstract)
- SONG G, LI H Y, YE N, et al, 2022. Types and features of diagenetic fluids in Shunbei No. 4 strike-slip fault zone in Shuntuoguole Low Uplift, Tarim Basin[J]. *Petroleum Geology & Experiment*, 44(4): 603-612. (in Chinese with English abstract)
- SONG Q, MA Q, DONG X J, et al, 2016. Sequence stratigraphic framework and sedimentary evolution of the Ordovician in northern Tarim Basin[J]. *Journal of Palaeogeography*, 18(5): 731-742. (in Chinese with English abstract)
- SONG Q, MA Q, LIU Y, et al, 2018. Sedimentary characteristics and distribution regularities of Ordovician carbonate grainstone shoals in Tabei area, NW China[J]. *Lithologic Reservoirs*, 30(1): 46-54. (in Chinese with English abstract)
- SONG Z P, LIU H K, ZHENG F, et al, 2023. Mechanical behavior and failure response characteristics of hard sandstones considering bedding dip angles[J]. *Coal Geology & Exploration*, 51(12): 167-175. (in Chinese with English abstract)
- SUN D S, LV H T, WANG L J, et al, 2018. Determination of the in-situ stress state at 7 km depth under Tarim Basin by ASR and DITH methods[J]. *Chinese Journal of Rock Mechanics and Engineering*, 37(2): 383-391. (in Chinese with English abstract)
- WALLS J D, DVORKIN J, 1994. Measured and calculated horizontal stresses in the Travis Peak Formation[J]. *SPE Formation Evaluation*, 9(4): 259-263.
- WANG B, ZHAO Y Q, HE S, et al, 2020. Hydrocarbon accumulation stages and their controlling factors in the northern Ordovician Shunbei 5 fault zone, Tarim Basin[J]. *Oil & Gas Geology*, 41(5): 965-974. (in Chinese with English abstract)
- WANG W B, FU H, LÜ L R, et al, 2021. Sequence model of Ordovician carbonate strata in Shunbei area, Tarim basin, and its significance[J]. *Acta Sedimentologica Sinica*, 39(6): 1451-1465. (in Chinese with English abstract)
- WANG W J, LI D Q, JIN J B, et al, 2022. Technical problems and measures of wellbore stability of broken formation in Shunbei oil and gas field[J]. *Science Technology and Engineering*, 22(13): 5205-5212. (in Chinese with English abstract)
- WANG Y W, CHEN H H, CAO Z C, et al, 2023. Controlling effects of fluid activity on reservoir formation in Shunbei area[J]. *Fault-block Oil & Gas Field*, 30(1): 44-51. (in Chinese with English abstract)
- WANG Y X, WANG B, GU Y, et al, 2023. Coupling relationship between fluid transformation and oil and gas filling of middle lower Ordovician in Shunbei area of Tarim Basin[J]. *Science Technology and Engineering*, 23(1): 66-76. (in Chinese with English abstract)
- WONG R H C, CHAU K T, WANG P, 1996. Microcracking and grain size effect in Yuen Long marbles[J]. *International Journal of Rock Mechanics and Mining Sciences & Geomechanics Abstracts*, 33(5): 479-485.
- WU B L, 2001. Boit's effective stress coefficient evaluation: static and dynamic approaches[C]//Proceedings of the ISRM International Symposium - 2nd Asian Rock Mechanics Symposium. Beijing: ISRM: 369-372.
- WU Q Q, LI J R, CAO F, et al, 2019. Characteristics of fault-karst carbonate reservoirs in the Shunbei No. 1 well block, Tarim basin[J]. *Carsologica Sinica*, 38(3): 444-449. (in Chinese with English abstract)
- XIA Z L, LIU S G, SHI H X, et al, 2008. Experimental analysis of the rock mechanical properties of the fractured reservoir under formation conditions in the Central Iran Basin[J]. *Petroleum Geology & Experiment*, 30(1): 86-93. (in Chinese with English abstract)
- YANG H B, WU Y Y, 2011. The experimental analysis of microstructure and mechanical properties of tight reservoir rocks[J]. *Complex Hydrocarbon Reservoirs*, 4(3): 10-15. (in Chinese with English abstract)
- YANG Q, SUN J, JIA Y X, et al, 2017. Experimental study on rock mechanics of reservoir Nanchang 8 in Ordos Basin[J]. *Petroleum Geology and Engineering*, 31(4): 100-103. (in Chinese with English abstract)
- YE G Q, CAO H, GAO Q, et al, 2019. Numerical simulation study on the influence of particle proportion on rock mechanics characteristics[J]. *Journal of Geomechanics*, 25(6): 1129-1137. (in Chinese with English abstract)
- YIN X Y, MA N, MA Z Q, et al, 2018. Review of in-situ stress prediction technology[J]. *Geophysical Prospecting for Petroleum*, 57(4): 488-504. (in Chinese with English abstract)
- ZENG L B, LI Z X, SHI C E, et al, 2007. Characteristics and origin of fractures in the extra low-permeability sandstone reservoirs of the Upper Triassic Yanchang Formation in the Ordos basin[J]. *Acta Geologica Sinica*, 81(2): 174-180. (in Chinese with English abstract)
- ZHANG G S, 2005. Characteristics of fractures in the tight sandstone reservoirs of Xujiahe Formation in West Sichuan Depression[J]. *Natural Gas Industry*, 25(7): 11-13, 26. (in Chinese with English abstract)
- ZHANG Y Y, LI D Q, GAO S Y, et al, 2022. Analysis on influencing factors of wellbore instability of Ordovician fractured formation in Shunbei Oil and Gas Field[J]. *Fault-Block Oil & Gas Field*, 29(2): 256-260. (in Chinese with English abstract)
- ZHANG Y, MAO Q Y, LI H Y, et al, 2023. Characteristics and practical application of ultra-deep fault-controlled fractured-cavity type reservoir in central Shunbei area[J]. *China Petroleum Exploration*, 28(1): 1-13. (in Chinese with English abstract)
- ZHAO J Y, JI D S, WU J, et al, 2022. Research on rock mechanics parameters of the Jurassic-Cretaceous reservoir in the Sikeshu sag, Junggar Basin,

- China[J]. Journal of Geomechanics, 28(4): 573-582. (in Chinese with English abstract)
- ZHAO N, WANG L, ZHANG L, et al, 2022. Mechanical properties and fracturing characteristics of tight sandstones based on granularity classification: a case study of Permian Lower Shihezi Formation, Ordos Basin[J]. Petroleum Geology & Experiment, 44(4): 720-729, 738. (in Chinese with English abstract)
- ZHAO R, ZHAO T, LI H L, et al, 2019. Fault-controlled fracture-cavity reservoir characterization and main-controlling factors in the Shunbei Hydrocarbon Field of Tarim Basin[J]. Special Oil and Gas Reservoirs, 26(5): 8-13. (in Chinese with English abstract)
- ZHAO Y Q, 2022. The fourth-order sequence stratigraphic division and geological significance of Ordovician Yingshan Formation in Shunbei—Shunnan area, Tarim Basin, China[J]. Journal of Chengdu University of Technology (Science & Technology Edition), 49(4): 454-467. (in Chinese with English abstract)
- ZHAO Z H, LIU Z N, PU H, et al, 2018. Effect of thermal treatment on brazilian tensile strength of granites with different grain size distributions[J]. Rock Mechanics and Rock Engineering, 51(4): 1293-1303.
- ZHU X X, ZHAO R, ZHAO T, 2023. Characteristics and control effect on reservoir and accumulation of strike-slip segments in Shunbei No. 1 fault zone, Tarim Basin[J]. Lithologic Reservoirs, 35(5): 131-138. (in Chinese with English abstract)
- ### 附中文参考文献
- 卜旭强, 王来源, 朱莲花, 等, 2023. 塔里木盆地顺北油气田奥陶系断控缝洞型储层特征及成藏模式[J]. 岩性油气藏, 35(3): 152-160.
- 陈平, 能源, 吴鲜, 等, 2023. 塔里木盆地顺北5号走滑断裂带分段特征及构造演化[J]. 新疆石油地质, 44(1): 33-42.
- 陈绍杰, 郭宇航, 黄万朋, 等, 2017. 粒度对红砂岩力学性质影响规律与机制试验研究[J]. 山东科技大学学报(自然科学版), 36(6): 8-14.
- 陈雨霖, 唐军, 2022. 新疆塔里木盆地托甫台地区碳酸盐岩储层缝洞测井评价[J]. 工程地球物理学报, 19(5): 689-698.
- 邓尚, 李慧莉, 张仲培, 等, 2018. 塔里木盆地顺北及邻区主干走滑断裂带差异活动特征及其与油气富集的关系[J]. 石油与天然气地质, 39(5): 878-888.
- 丁文龙, 尹帅, 王兴华, 等, 2015. 致密砂岩气储层裂缝评价方法与表征[J]. 地学前缘, 22(4): 173-187.
- 傅海成, 张承森, 赵良孝, 等, 2006. 塔里木盆地轮南奥陶系碳酸盐岩储层类型测井识别方法[J]. 西安石油大学学报(自然科学版), 21(5): 38-41.
- 高晨阳, 赵福海, 高莲凤, 等, 2023. 基于构造应变分析的裂缝预测方法及其应用[J]. 地质力学学报, 29(1): 21-33.
- GB/T 50266—2013. 2013. 工程岩体试验方法标准[S]. 北京, 中国计划出版社.
- 葛洪魁, 林英松, 王顺昌, 1998. 地应力测试及其在勘探开发中的应用[J]. 石油大学学报(自然科学版), 22(1): 94-99.
- 葛洪魁, 陈颀, 林英松, 2001. 岩石动态与静态弹性参数差别的微观机理[J]. 石油大学学报(自然科学版), 25(4): 34-36.
- 郭思强, 2020. 大庆油田 T30 井区扶余油层致密储层岩石力学参数建模[J]. 大庆石油地质与开发, 39(5): 169-174.
- 郭禹希, 秦严, 王海, 等, 2022. 粒径对破碎岩石力学性质影响模型试验研究[J]. 科学技术与工程, 22(11): 4489-4496.
- 韩强, 云露, 蒋华山, 等, 2021. 塔里木盆地顺北地区奥陶系油气充注过程分析[J]. 吉林大学学报(地球科学版), 51(3): 645-658.
- 韩振华, 张路青, 周剑, 等, 2019. 矿物粒径对花岗岩单轴压缩特性影响的试验与模拟研究[J]. 工程地质学报, 27(3): 497-504.
- 侯龙飞, 杨春和, 郭印同, 等, 2020. 缝洞型碳酸盐岩近井筒裂缝转向模拟研究[J]. 科学技术与工程, 20(27): 11080-11086.
- 胡广强, 白彬珍, 柯珂, 2017. 顺北区块辉绿岩井段井壁稳定性分析[J]. 中国海上油气, 29(5): 119-125.
- 黄荣樽, 白家祉, 周煜辉, 等, 1993. 斜直井井壁张性裂纹的位置及走向与井眼压力的关系[J]. 石油钻采工艺, 15(5): 7-11.
- 贾焰然, 石军太, 李星浩, 等, 2021. 低渗致密气井分类评价方法研究: 以长庆子洲气田为例[J]. 地质与勘探, 57(3): 647-655.
- 蒋明镜, 白闰平, 刘静德, 等, 2013. 岩石微观颗粒接触特性的试验研究[J]. 岩石力学与工程学报, 32(6): 1121-1128.
- 焦方正, 2018. 塔里木盆地顺北特深碳酸盐岩断溶体油气藏发现意义与前景[J]. 石油与天然气地质, 39(2): 207-216.
- 金峰, 朱秀香, 余一欣, 等, 2023. 塔里木盆地顺北地区 13 号走滑断裂带发育特征[J]. 大地构造与成矿学, 47(1): 54-65.
- 康瀚, 2013. 不同粒径砂岩三轴压缩力学特性试验研究[J]. 路基工程(6): 94-96, 101.
- 孔亮, 彭仁, 2011. 颗粒形状对类砂土力学性质影响的颗粒流模拟[J]. 岩石力学与工程学报, 30(10): 2112-2119.
- 李树博, 姜伟, 张效恭, 等, 2019. 塔里木盆地巴楚凸起 H 气田奥陶系裂缝主控因素及演化序列研究[J]. 地质力学学报, 25(4): 518-526.
- 李智武, 罗玉宏, 刘树根, 等, 2005. 川东北地区地层条件下致密储层力学性质实验分析[J]. 矿物岩石, 25(4): 52-60.
- 刘宝增, 2020. 塔里木盆地顺北地区油气差异聚集主控因素分析: 以顺北 1 号、顺北 5 号走滑断裂带为例[J]. 中国石油勘探, 25(3): 83-95.
- 刘广, 荣冠, 彭俊, 等, 2013. 矿物颗粒形状的岩石力学特性效应分析[J]. 岩土工程学报, 35(3): 540-550.
- 刘建章, 蔡忠贤, 滕长宇, 等, 2023. 塔里木盆地顺北地区克拉通内走滑断裂带中-下奥陶统储集体方解石脉形成及其与油气充注耦合关系[J]. 石油与天然气地质, 44(1): 125-137.
- 刘荣和, 冯文光, 龙玲, 等, 2008. 致密碳酸盐岩岩石力学与声学实验研究[J]. 大庆石油地质与开发, 27(6): 131-135.
- 刘圣鑫, 王宗秀, 张林炎, 等, 2018. 基于纳米压痕的页岩微观力学性质分析[J]. 实验力学, 33(6): 957-968.
- 刘圣鑫, 王宗秀, 张林炎, 等, 2019. 页岩微观组构特征对复杂裂缝网络形成的影响[J]. 采矿与安全工程学报, 36(2): 420-428.
- 柳洲, 康志宏, 周磊, 等, 2014. 缝洞型碳酸盐岩油藏剩余油分布模式: 以塔河油田六七区为例[J]. 现代地质, 28(2): 369-378.
- 鲁新便, 胡文革, 汪彦, 等, 2015. 塔河地区碳酸盐岩断溶体油藏特征与开发实践[J]. 石油与天然气地质, 36(3): 347-355.
- 吕海涛, 韩俊, 张继标, 等, 2021. 塔里木盆地顺北地区超深碳酸盐岩断溶体发育特征与形成机制[J]. 石油实验地质, 43(1): 14-22.
- 马乃拜, 马新平, 杜伟维, 等, 2019. 顺北一区奥陶系碳酸盐岩储层

- 发育特征与预测[J]. 内蒙古石油化工, 45(7): 106-112.
- 马秋峰, 秦跃平, 周天白, 等, 2019. 基于颗粒接触理论的岩石压实阶段本构模型[J]. 中南大学学报(自然科学版), 50(8): 1941-1948.
- 马永生, 何治亮, 赵培荣, 等, 2019. 深层—超深层碳酸盐岩储层形成机理新进展[J]. 石油学报, 40(12): 1415-1425.
- 宁超众, 孙龙德, 胡素云, 等, 2021. 塔里木盆地哈拉哈塘油田奥陶系缝洞型碳酸盐岩储层岩溶类型及特征[J]. 石油学报, 42(1): 15-32.
- 漆立新, 2020. 塔里木盆地顺北超深溶解体油藏特征与启示[J]. 中国石油勘探, 25(1): 102-111.
- 漆立新, 丁勇, 2023. 塔里木盆地顺北地区东西部海相油气成藏差异[J]. 石油实验地质, 45(1): 20-28.
- 尚凯, 郭娜, 曹自成, 等, 2017. 塔里木盆地塔中北坡奥陶系一间房组储集层主控因素分析[J]. 海相油气地质, 22(1): 39-46.
- 史江涛, 郝君明, 王小雷, 2022. 塔河地区奥陶系鹰山组储层特征及其主控因素[J]. 吉林大学学报(地球科学版), 52(2): 348-362.
- 舒红林, 仇凯斌, 李庆飞, 等, 2021. 页岩气地质力学特征评价方法: 中国南海相强改造区山地页岩地质力学特征[J]. 天然气工业, 41(S1): 1-13.
- 宋刚, 李海英, 叶宁, 等, 2022. 塔里木盆地顺托果勒低隆起顺北4号走滑断裂带成岩流体类型及活动特征[J]. 石油实验地质, 44(4): 603-612.
- 宋倩, 马青, 董旭江, 等, 2016. 塔里木盆地北部地区奥陶系层序地层格架与沉积演化[J]. 古地学报, 18(5): 731-742.
- 宋倩, 马青, 刘莹, 等, 2018. 塔北地区奥陶系碳酸盐岩颗粒滩沉积特征及分布规律[J]. 岩性油气藏, 30(1): 46-54.
- 宋战平, 刘洪珂, 郑方, 等, 2023. 考虑层理倾角的硬质砂岩力学行为及破裂响应特征[J]. 煤田地质与勘探, 51(12): 167-175.
- 孙东生, 吕海涛, 王连捷, 等, 2018. ASR和DITF法综合确定塔里木盆地7 km深部地应力状态[J]. 岩石力学与工程学报, 37(2): 383-391.
- 王斌, 赵永强, 何生, 等, 2020. 塔里木盆地顺北5号断裂带北段奥陶系油气成藏期次及其控制因素[J]. 石油与天然气地质, 41(5): 965-974.
- 王伟吉, 李大奇, 金军斌, 等, 2022. 顺北油气田破碎性地层井壁稳定技术难题与对策[J]. 科学技术与工程, 22(13): 5205-5212.
- 王文博, 傅恒, 闫廖然, 等, 2021. 塔里木盆地顺北地区奥陶系碳酸盐岩层序模式及其意义[J]. 沉积学报, 39(6): 1451-1465.
- 王玉伟, 陈红汉, 曹自成, 等, 2023. 顺北地区流体活动对储层形成的控制作用[J]. 断块油气田, 30(1): 44-51.
- 王昱翔, 王斌, 顾忆, 等, 2023. 塔里木盆地顺北地区中下奥陶统流体改造与油气充注耦合关系[J]. 科学技术与工程, 23(1): 66-76.
- 伍齐乔, 李景瑞, 曹飞, 等, 2019. 顺北1井区奥陶系溶解体油藏岩溶发育特征[J]. 中国岩溶, 38(3): 444-449.
- 夏在连, 刘树根, 时华星, 等, 2008. 中伊朗盆地地层条件下裂缝性储层岩石力学性质实验分析[J]. 石油实验地质, 30(1): 86-93.
- 杨海博, 武云云, 2011. 致密储层岩石的微观结构和力学性质试验分析[J]. 复杂油气藏, 4(3): 10-15.
- 杨琦, 孙洁, 贾昱昕, 等, 2017. 鄂尔多斯盆地南部8储层岩石力学实验研究[J]. 石油地质与工程, 31(4): 100-103.
- 叶功勤, 曹函, 高强, 等, 2019. 颗粒对比对岩石力学特征影响的数值模拟研究[J]. 地质力学学报, 25(6): 1129-1137.
- 印兴耀, 马妮, 马正乾, 等, 2018. 地应力预测技术的研究现状与进展[J]. 石油物探, 57(4): 488-504.
- 曾联波, 李忠兴, 史成恩, 等, 2007. 鄂尔多斯盆地上三叠统延长组特低渗透砂岩储层裂缝特征及成因[J]. 地质学报, 81(2): 174-180.
- 张贵生, 2005. 川西坳陷须家河组致密砂岩储层裂缝特征[J]. 天然气工业, 25(7): 11-13, 26.
- 张亚云, 李大奇, 高书阳, 等, 2022. 顺北油气田奥陶系破碎性地层井壁失稳影响因素分析[J]. 断块油气田, 29(2): 256-260.
- 张煜, 毛庆言, 李海英, 等, 2023. 顺北中部超深层断控缝洞型油气藏储集体特征与实践应用[J]. 中国石油勘探, 28(1): 1-13.
- 赵进雍, 冀冬生, 吴见, 等, 2022. 准噶尔盆地四棵树凹陷侏罗系—白垩系储层岩石力学参数研究[J]. 地质力学学报, 28(4): 573-582.
- 赵宁, 王亮, 张磊, 等, 2022. 基于粒径分类的致密砂岩力学特性及破坏特征研究: 以鄂尔多斯盆地二叠系下石盒子组为例[J]. 石油实验地质, 44(4): 720-729, 738.
- 赵锐, 赵腾, 李慧莉, 等, 2019. 塔里木盆地顺北油气田断控缝洞型储层特征与主控因素[J]. 特种油气藏, 26(5): 8-13.
- 赵永强, 2022. 塔里木盆地顺北—顺南地区鹰山组四级层序地层划分及地质意义[J]. 成都理工大学学报(自然科学版), 49(4): 454-467.
- 朱秀香, 赵锐, 赵腾, 2023. 塔里木盆地顺北1号断裂带走滑分段特征与控储控藏作用[J]. 岩性油气藏, 35(5): 131-138.